


Tunneling noise and defects in exfoliated hexagonal boron nitride

Cite as: AIP Advances 9, 105218 (2019); doi: 10.1063/1.5126129

Submitted: 29 August 2019 • Accepted: 14 October 2019 •

Published Online: 22 October 2019



Xuanhan Zhao,¹ Panpan Zhou,¹ Liyang Chen,² Kenji Watanabe,³ Takashi Taniguchi,³
and Douglas Natelson^{1,4,5,a)} 

AFFILIATIONS

¹Department of Physics and Astronomy, Rice, University, Houston, Texas 77005, USA

²Applied Physics Program, Smalley-Curl Institute, Rice University, 6100 Main Street, Houston, Texas 77005, USA

³National Institute for Materials Science, 1-1 Namiki, Tsukuba, Ibaraki 305-0044, Japan

⁴Department of Electrical and Computer Engineering, Rice University, 6100 Main Street, Houston, Texas 77005, USA

⁵Department of Materials Science and NanoEngineering, Rice University, 6100 Main Street, Houston, Texas 77005, USA

^{a)}Corresponding author: natelson@rice.edu

ABSTRACT

Hexagonal boron nitride (hBN) has become a mainstay as an insulating barrier in stackable nanoelectronics because of its large bandgap and chemical stability. At mono- and bilayer thicknesses, hBN can function as a tunnel barrier for electronic spectroscopy measurements. Noise spectroscopy is of particular interest, as noise can be a sensitive probe for electronic correlations not detectable by first-moment current measurements. In addition to the expected Johnson-Nyquist thermal noise and nonequilibrium shot noise, low frequency (<100 kHz) noise measurements in Au/hBN/Au tunneling structures as a function of temperature and bias reveal the presence of thermally excited dynamic defects, as manifested through a flicker noise contribution at high bias that freezes out as temperature is decreased. In contrast, broad-band high frequency (~250MHz – 580MHz) measurements on the same device show shot noise with no flicker noise contribution. The presence of the flicker noise through multiple fabrication approaches and processing treatments suggests that the fluctuators are in the hBN layer itself. Device-to-device variation and the approximate $1/f$ dependence of the flicker noise constrain the fluctuator density to on the order of a few per square micron.

© 2019 Author(s). All article content, except where otherwise noted, is licensed under a Creative Commons Attribution (CC BY) license (<http://creativecommons.org/licenses/by/4.0/>). <https://doi.org/10.1063/1.5126129>

Hexagonal boron nitride (hBN) is a van der Waals layered material with a large bandgap, high dielectric breakdown strength, and strong chemical stability. It has become a critical component in the burgeoning field of 2D materials, as a substrate with minimal charge disorder,¹ as clean encapsulant for layered materials,² and as a tunneling barrier³ for a variety of candidate devices. One potential application of hBN is as a mechanically placeable tunnel barrier for electronic spectroscopy. Signatures of defects in hBN tunnel barriers have been seen in transport measurements,⁴ with indications that these defects can trap charge and provide resonant tunneling pathways. Optical spectroscopy has also shown that point defects in hBN are candidate quantum emitters.^{5,6}

Electronic noise in transport, fluctuations about the mean value of the current through or voltage across a system, has

proven to be a powerful technique in identifying electronic transport processes and the role of defects. One intrinsic noise process is Johnson-Nyquist noise, the thermodynamic consequence of fluctuations of the occupation number of the electronic states at finite temperature, which can be used as a means of probing the absolute electronic temperature. Shot noise appears in systems driven out of equilibrium as a consequence of the discreteness of charge carriers. Electronic shot noise was first discovered⁷ by considering current fluctuations in vacuum tubes. When the transport of carriers of charge e is governed by Poisson statistics, the mean square current fluctuations per unit bandwidth (A^2/Hz) are given by

$$S_I = 2e\langle I \rangle \quad (1)$$

where S_I is the current fluctuation spectral density, $\langle I \rangle$ is the time-averaged current and e is the electron charge. Shot noise changes with temperature as defined by the well-known form⁸

$$S_I = F \cdot 2eI \coth\left(\frac{eV}{2k_B T}\right) + (1 - F) \cdot 4k_B T G \quad (2)$$

where V is the applied bias, T is the environmental temperature, and G is the zero-bias conductance of the device. The magnitude of the measured shot noise does not always match the Poissonian result, and is instead described in the high bias limit using the Fano factor, $F = \frac{S_{I, \text{measured}}}{2eI}$. At zero bias, Equation 2 is constructed to reduce to the Johnson-Nyquist noise, $4k_B T G$ at zero bias voltage, and at high voltage bias ($eV \gg 2k_B T$), the noise increases linearly with bias as $F \cdot 2eI$. The Fano factor can be suppressed to zero in macroscopic conductors through inelastic electron-phonon scattering.⁹ When transmission is through only a small number of electronic channels, the Fano factor can reflect the “fingerprint” of the transmittances of those channels.¹⁰ In the limit of a single channel with transmittance much smaller than 1, $F \rightarrow 1$. Electronic correlation effects can modify F , as in the edge-state tunneling of fractionally charged quasiparticles in the fractional quantum Hall regime,¹¹ or in superconductor systems with charge pairing.¹² Inelastic phonon effects,¹³ charge trapping defects,¹⁴ and space charge interactions¹⁵ can also modify Fano factors. Defect-free hBN junction structures are expected to function as conventional tunnel barriers. Because one can treat a conventional large-area tunnel junction as a parallel combination of many low-transmittance channels, and the Fano factors of these structures are expected to be 1. Both Johnson-Nyquist and shot noise power spectral densities are expected to be “white”, independent of frequency, f , over a very broad range of frequencies, set by the temperature and the carrier traversal time, respectively.

“Flicker” noise due to slow temporal fluctuations in device resistance is a very common extrinsic effect in conductive devices.¹⁶ The voltage noise power spectral density, S_V , for flicker noise is quadratic in the applied dc current since it originates from resistance fluctuations. Often the frequency dependence of this noise is approximately $1/f$, due to ensemble-averaging of the contributions of a large number of fluctuators each with its own characteristic timescale. When the number of fluctuators is small, pronounced deviations from $1/f$ dependence of the spectral density are observed, with a single fluctuator leading to a Lorentzian spectrum.¹⁷

We report investigations of shot noise in simple hBN-based tunneling devices with metal source and drain electrodes, measured using both a low-frequency cross-correlation method and a lock-in based radio frequency measurement technique. Low-frequency measurements show the presence of fluctuating defects at higher temperatures, presumably in the hBN barrier, leading to a large flicker noise $1/f$ contribution to the noise signal. There is variability from device to device about the magnitude of the flicker noise and its precise functional form and temperature dependence, consistent with noise originating from a comparatively small number of fluctuators. The frequency dependence and device-to-device variability constrain the defect density to a few per square micron. Device annealing under the mild conditions required to preserve electrode integrity has comparatively little effect on these results. The high frequency measurements, in contrast, are consistent with shot noise

alone. These results show that defects in hBN may be a noise source in certain device applications.

To fabricate the Au/hBN/Au tunnel junctions, shown in Figure 1(a), we have adopted a widely-used wet transfer method, previously designed for picking 2D materials from SiO₂/Si wafers using adhesive tape. First, hBN flakes are exfoliated onto 300 nm SiO₂/Si wafers using adhesive tape. Then, the carrier substrate with the target flakes is spin coated with poly-methyl-methacrylate (PMMA) 495 A4 at 3000 rpm for 1 minute and baked for 3 minutes at 180 °C on a hot plate. Next, a NITTO tape with 2 mm by 2 mm window hole is placed on top of the PMMA with the hole aligned with the target flakes. The SiO₂ layer on the substrate is etched away by soaking the whole substrate in 1M KOH solution for 2 hours at 50 °C followed by soaking in deionized water, freeing the PMMA that carries the target flakes from the substrate. The hBN is then transferred onto a target substrate with lithographically patterned bottom electrodes by pushing the target-flake-carrying-surface of the PMMA into contact by micro-manipulator alignment under a microscope. The area of each tunnel junction is approximately 1 μm^2 , set by the width of the top and bottom electrodes.

After fabrication, the tunneling current and differential resistance, dV/dI , shown in Figure 1(c, d), are measured via standard lock-in techniques. The device measured shows rather Ohmic I - V curves over the measured bias range, and with very little temperature dependence. Consistent with the I - V characteristics, the changes in dV/dI are also small, suggesting the defect density is comparably low, with no large contributions to conduction by resonant tunneling through defects, for example.

Figure 1(b) is a schematic electrical circuit diagram of the low-frequency noise measurement setup. A tunable voltage source with LC filters applies a clean dc bias current to the sample loaded inside a cryostat. The voltage and its fluctuations across the sample is amplified by two low-noise voltage preamplifiers chains (NF Corp. LI-75, 100 \times gain, followed by Stanford Research SR560, 100 \times gain) independently. Each amplified voltage as a function of time is recorded by a high-speed digitizer (NI-PCI5122) at a sampling rate of 5 MHz within 10 ms for each time series. The data from the two amplifier chains are cross-correlated to mitigate the effects of amplifier input noise, and each recorded voltage noise power spectrum S_V is a result of 4000 averages. After cross-correlation the resulting spectra are then converted into the units of current noise spectral density (A^2/Hz) using the measured differential resistance, $R_S = dV/dI$, at each bias (Figure 2(a-d)).

The suppression of voltage noise power at higher frequencies is due to parasitic capacitance to ground C , dominantly in the measurement wiring. The solid lines are the result of fitting to a capacitive model, where the measured noise $S_{V, \text{meas}}(\omega)$ is related to the true source noise $S_V(\omega) \sim \text{constant}$ (white in frequency) by $S_{V, \text{meas}}(\omega) = S_V / (1 + (\tau_{RC}\omega)^2)$, where $\tau_{RC} = R_S C$ is a capacitive time constant, where R_S is the differential resistance at given bias. We find that τ_{RC} at each temperature is consistent with a constant capacitance and the measured R_S at each bias.

Shown in Figure 2(e-g) are the extracted current noise data $S_I = S_V/R_S^2$ as a function of bias for relatively low biases and several temperatures, compared with the theoretical values calculated using Eq. 2. The Johnson-Nyquist zero-bias thermal level, the slope at higher biases, and the curvature about zero bias are all consistent with Equation 2 with a Fano factor of 1.

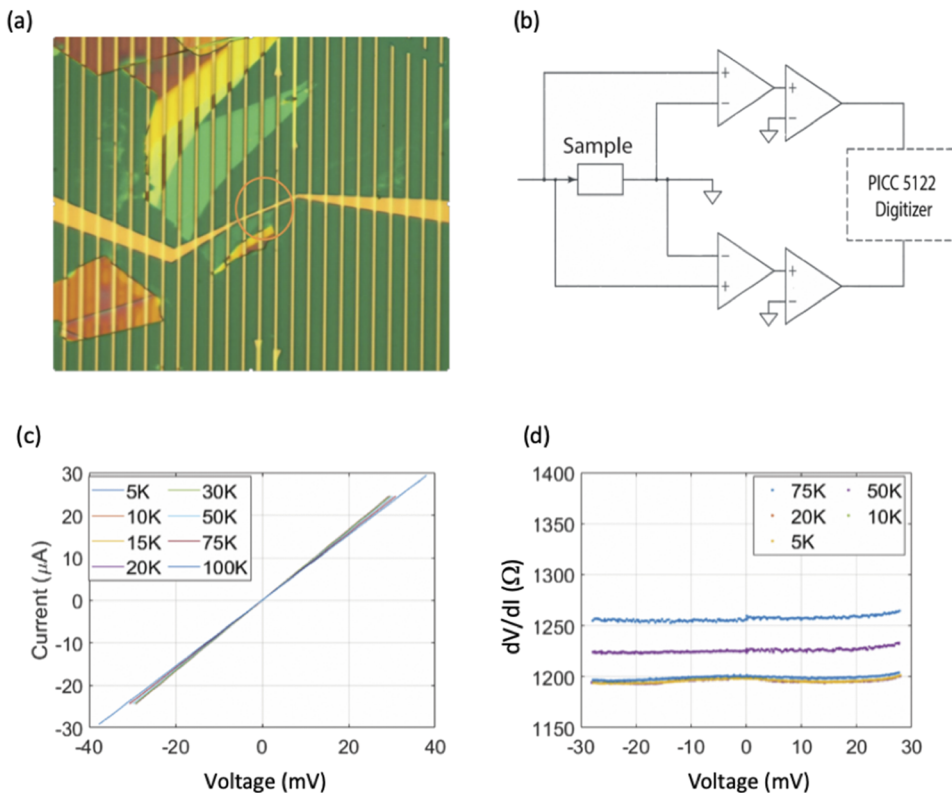


FIG. 1. (a) An optical image of hBN flake after transfer onto underlying electrodes (vertical lines), and after lithographic fabrication of top electrodes (roughly horizontal feature). The image is taken with a green filter for better optical contrast. Orange circle indicates location of tunnel junction. (b) Schematic diagram of the low-frequency noise measurement setup. (c) I - V characteristics of the device in (a) acquired at different temperatures. (d) Corresponding dV/dI measurements of the device, acquired through standard lock-in methods.

It is evident from Fig. 2(c, d), however, that at higher temperatures and higher bias currents, the spectrum deviates markedly from the capacitively-attenuated white noise expectation of Johnson-Nyquist and shot noise, with a clear onset of an anomalous flicker-like $1/f$ component. Below 20 K there are barely any signs of this anomalous noise, and the capacitive fits match very well with the raw spectra. Starting from 20 K, the low-frequency noise become more obvious as temperature increases. The magnitude of this low-frequency noise, above 75 K, becomes large enough to affect the high frequency part of the spectrum and obstruct the extraction of accurate of the shot noise using our model. This device is representative of several, and comparatively simple phenomenologically. We find a flicker noise spectral component in a variety of Au/hBN/Au junction configurations. The shape of the flicker noise spectrum in particular devices often deviates from a simple $1/f$ shape as the temperature is varied, though usually without clear Lorentzian peaks that allow simple fitting in terms of individual fluctuators.¹⁷ Generally, the flicker noise is larger at higher temperatures within a given device, though we have also observed a nonmonotonic temperature dependence.

Because of the device-to-device variation, it is challenging to extract detailed quantitative information about the fluctuating defects. If we assume that the $1/f$ -like spectrum results from the superposition of Lorentzian spectra of individual fluctuators with characteristic lifetimes spread out over the measurement bandwidth, modeling shows that around seven fluctuators (of identical magnitudes but distributed lifetimes) are needed to reproduce a $1/f$ -like

spectrum. The variation in flicker noise magnitude and temperature dependence in the devices measured suggests that the number of fluctuators must not be much larger than this, or one would expect universality of response across the devices due to ensemble averaging. This suggests a fluctuator defect density on the order of 7 per μm^2 . The variation in temperature dependence likewise implies characteristic energy scales for the fluctuators on the order of the temperature scale, several meV.

To test for whether the noise originates due to the fabrication process, we also fabricated devices using a dry transfer process based on polydimethylsiloxane (PDMS) pick-up. We observe similar flicker noise in devices prepared by both wet and dry transfer procedures (as seen in [supplementary material](#)), with post-fabrication annealing in forming gas (20% H_2 , 80% N_2) up to 200 °C for 4 hours. This ubiquity of flicker response, independent of processing, suggests that the fluctuations originate in the hBN layer itself.

In the same device as in Fig. 2, we perform a comparison with a broad-band RF measurement of shot noise, employed previously in Au/hBN/Au junctions.¹⁹ The broadband method^{20,21} (Figure 3(a)) modulates the bias current through the device and uses a lock-in amplifier to detect the resulting change in the integrated noise power over a bandwidth from 250 MHz to 580 MHz. This provides a check on whether defects are present in sufficient quantity with relaxation timescales in the radio frequency range to be problematic for noise spectroscopy. As was observed previously,¹⁹ the measured noise evolves consistently with the prediction of Eq. 2 (with an overall prefactor related to the RF pickup efficiency of the measurement

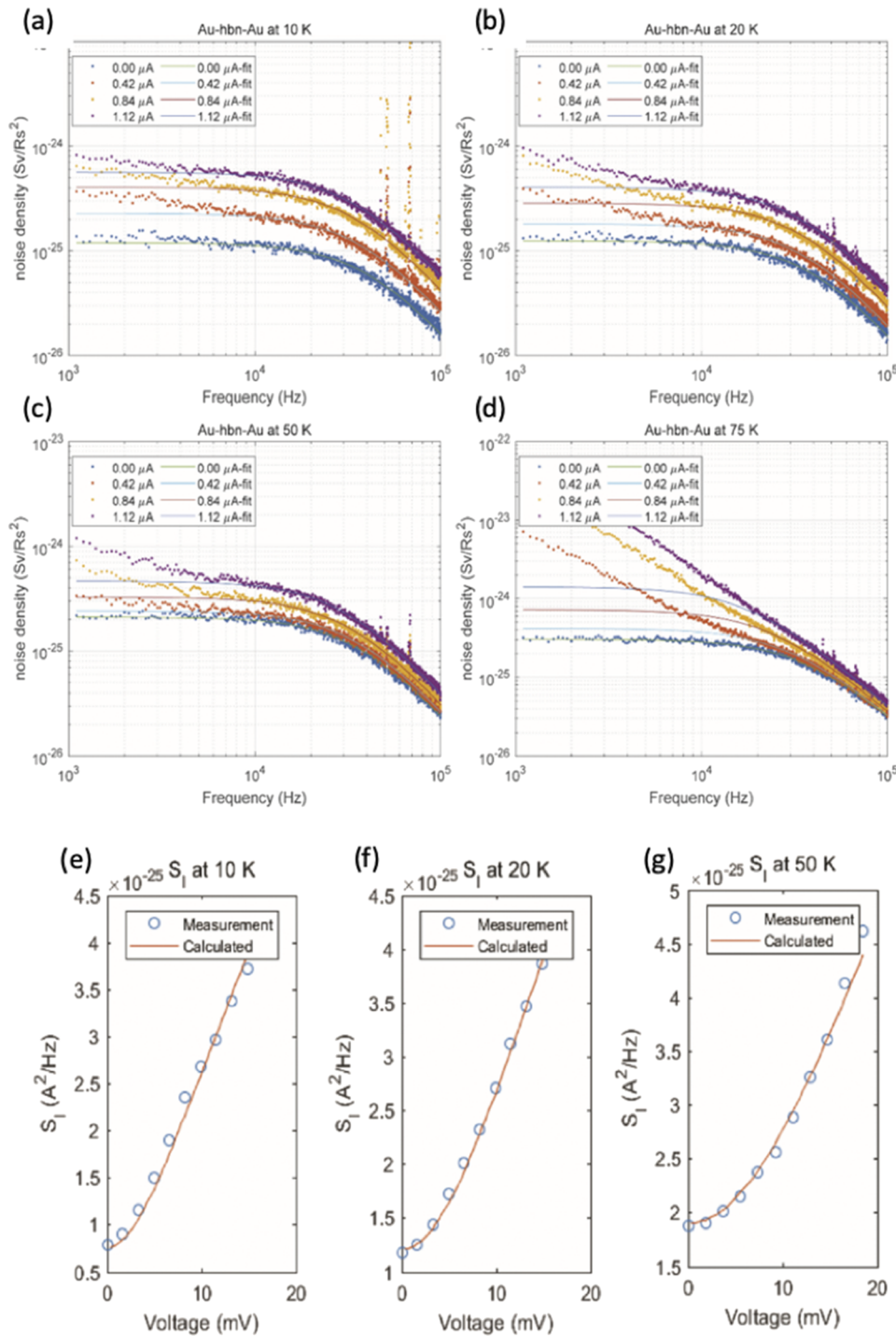


FIG. 2. Shot noise measurement on Au/hBN/Au junctions using low frequency measurement setup. (a-d) Current noise spectral density (voltage noise spectral density divided by (differential resistance)²) of after cross-correlation at specific temperatures and several dc bias currents, and the fits using the constant RC model to describe the capacitive roll-off. Only a few biases are shown for clarity. The presence of a large flicker noise ($1/f$ -like) contribution at higher temperatures and higher biases is clear. (e-g) The extracted current noise magnitude compared with the value calculated based on Eq. 2 and sample resistance at different temperatures. In the absence of the flicker noise contribution, the remaining signal is quantitatively consistent with the expectations of Johnson-Nyquist and shot noise with a Fano factor of 1.

probe). As shown in Fig. 3, the RF noise at 50 K, 75 K, and 100 K show no sign of a flicker noise contribution, which would manifest as a large quadratic-in-bias-current contribution to the noise. These measurements show that the defects responsible for the flicker

noise have characteristic fluctuation timescales slow compared to the nanosecond regime.

We have measured low-frequency noise in Au/hBN/Au tunnel junctions, and at temperatures above 10 K have found a large,

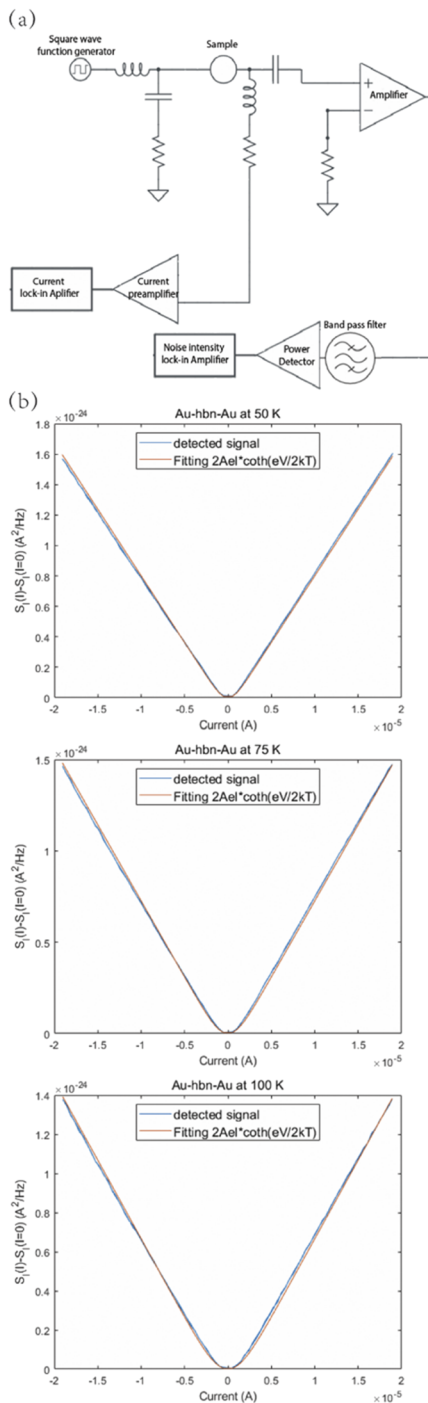


FIG. 3. (a) Radio-frequency noise measurement approach, which measures the change in integrated RF noise power from 250 MHz to 580 MHz when a bias current is turned on and off. (b) The bias-driven noise as a function of bias current for the device of Fig. 2. Over the same temperature range where low-frequency measurements show large flicker noise, the RF measurements show noise consistent with the expectations of finite-temperature shot noise as in Eq. 2, indicating that defect fluctuators do not contribute significantly to the current noise on nanosecond timescales.

temperature-dependent flicker noise contribution, in addition to conventional Johnson-Nyquist and shot noise. This indicates the presence of fluctuating defects in the junction, and the independence of this flicker noise to fabrication and processing details suggests that the defects are associated with the hBN itself. The frequency dependence and variability from device to device in frequency and temperature dependence constrain the fluctuator density to ~ 7 per μm^2 and energy scales of a few meV. Radio frequency investigations show that the fluctuators are not active on the nanosecond timescale. These observations imply that care must be taken in the use of hBN as a mechanically placeable tunnel barrier. Further investigations, such as combinations of tunneling with other spectroscopic techniques like electron paramagnetic resonance, could be helpful in further constraining the types and densities of microscopic defects that contribute to the flicker noise.

See [supplementary material](#) for examples of low-frequency noise spectra on additional devices, showing the presence of flicker noise.

XZ and DN acknowledge support from NSF Grant No. DMR-1704264 for financial support. PZ and LC contributed through data acquisition and analysis software, and along with some measurement hardware were supported by DOE BES award DE-FG02-06ER46337. K.W. and T.T. acknowledge support from the Elemental Strategy Initiative conducted by the MEXT, Japan, A3 Foresight by JSPS and the CREST (JPMJCR15F3), JST.

REFERENCES

- C. R. Dean, A. F. Young, I. Meric, C. Lee, L. Wang, S. Sorgenfrei, K. Watanabe, T. Taniguchi, P. Kim, K. L. Shepard, and J. Hone, *Nature Nanotechnology* **5**, 722 (2010).
- L. Wang, Z. Chen, C. R. Dean, T. Taniguchi, K. Watanabe, L. E. Brus, and J. Hone, *ACS Nano* **6**(10), 9314–9319 (2012).
- G.-H. Lee, Y.-J. Yu, C. Lee, C. Dean, K. L. Shepard, P. Kim, and J. Hone, *Applied Physics Letters* **99**(24), 243114 (2011).
- U. Chandni, K. Watanabe, T. Taniguchi, and J. P. Eisenstein, *Nano Letters* **15**(11), 7329–7333 (2015).
- N. R. Jungwirth and G. D. Fuchs, *Physical Review Letters* **119**(5), 057401 (2017).
- T. T. Tran, C. Elbadawi, D. Totonjian, C. J. Lobo, G. Grosso, H. Moon, D. R. Englund, M. J. Ford, I. Aharonovich, and M. Toth, *ACS Nano* **10**(8), 7331–7338 (2016).
- W. Schottky, *Annalen der Physik* **362**(23), 541–567 (1918).
- L. Spietz, K. W. Lehnert, I. Siddiqi, and R. J. Schoelkopf, *Science* **300**(5627), 1929–1932 (2003).
- Y. M. Blanter and M. Büttiker, *Physics Reports* **336**(1), 1–166 (2000).
- S. Datta, H. Ahmad, and M. Pepper, *Electronic Transport in Mesoscopic Systems* (Cambridge University Press, 1997).
- R. de-Picciotto, M. Reznikov, M. Heiblum, V. Umansky, G. Bunin, and D. Mahalu, *Nature* **389**(6647), 162–164 (1997).
- P. Dieleman, H. G. Bukkems, T. M. Klapwijk, M. Schicke, and K. H. Gundlach, *Physical Review Letters* **79**(18), 3486–3489 (1997).
- A. Mitra, I. Aleiner, and A. J. Millis, *Physical Review B* **69**(24), 245302 (2004).
- S. S. Safonov, A. K. Savchenko, D. A. Bagrets, O. N. Jouravlev, Y. V. Nazarov, E. H. Linfield, and D. A. Ritchie, *Physical Review Letters* **91**(13), 136801 (2003).
- A. Reklaitis and L. Reggiani, *Physical Review B* **62**(24), 16773–16776 (2000).
- M. B. Weissman, *Reviews of Modern Physics* **60**(2), 537–571 (1988).

¹⁷C. T. Rogers and R. A. Buhrman, [Physical Review Letters](#) **53**(13), 1272–1275 (1984).

¹⁸A. V. Kretinin, Y. Cao, J. S. Tu, G. L. Yu, R. Jalil, K. S. Novoselov, S. J. Haigh, A. Gholinia, A. Mishchenko, M. Lozada, T. Georgiou, C. R. Woods, F. Withers, P. Blake, G. Eda, A. Wirsig, C. Hucho, K. Watanabe, T. Taniguchi, A. K. Geim, and R. V. Gorbachev, [Nano Letters](#) **14**(6), 3270–3276 (2014).

¹⁹P. Zhou, W. J. Hardy, K. Watanabe, T. Taniguchi, and D. Natelson, [Applied Physics Letters](#) **110**(13), 133106 (2017).

²⁰M. Reznikov, M. Heiblum, H. Shtrikman, and D. Mahalu, [Physical Review Letters](#) **75**(18), 3340–3343 (1995).

²¹F. Wu, L. Roschier, T. Tsuneta, M. Paalanen, T. Wang, and P. Hakonen, [AIP Conference Proceedings](#) **850**(1), 1482–1483 (2006).